LA-UR-12-22587

Approved for public release; distribution is unlimited.

Title: Wind turbine blade fatigue tests: lessons learned and application to SHM system development

Author(s):
Taylor, Stuart G.
Farinholt, Kevin M.
Jeong, Hyomi
Jang, JaeKyung
Park, Gyu Hae
Todd, Michael D.
Farrar, Charles R.
Ammerman, Curtt N.

Intended for: European Workshop on Structural Health Monitoring, 2012-07-03/2012-07-06 (Dresden, ---, Germany)

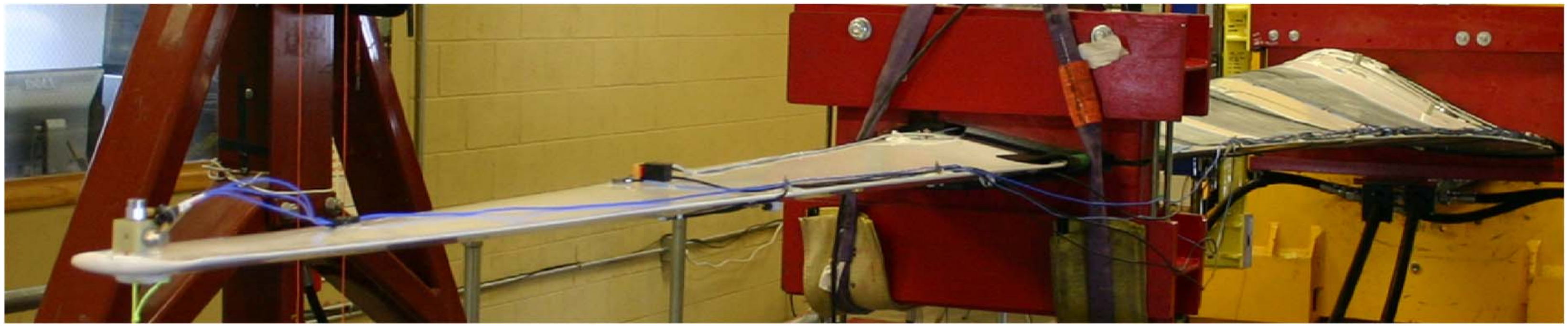

Wind turbine blade fatigue tests: lessons learned and application to SHM system development

Stuart. G. Taylor[1,5], Kevin M. Farinholt[2], Hyomi Jeong[3], JaeKyung Jang[3], Gyuhae Park[4], Michael D. Todd[1], Charles R. Farrar[5], and Curtt M. Ammerman[2]

1. Structural Engineering, University of California, San Diego, La Jolla, CA, USA
2. Applied Engineering Technology, Los Alamos National Laboratory, Los Alamos, NM USA
3. Engineering Institute – Korea, Chonbuk National University, Jeonju, Chonbuk, Korea
4. School of Mechanical Systems Engineering, Chonnam National University, Gwangju, South Korea
5. The Engineering Institute, Los Alamos National Laboratory, Los Alamos, NM, USA

European Workshop on Structural Health Monitoring
July 3-6, Dresden, Germany

Abstract

- This paper presents experimental results of several structural health monitoring (SHM) methods applied to a 9-meter CX-100 wind turbine blade that underwent fatigue loading. The blade was instrumented with piezoelectric transducers, accelerometers, acoustic emission sensors, and foil strain gauges. It underwent harmonic excitation at its first natural frequency using a hydraulically actuated resonant excitation system. The blade was initially excited at 25% of its design load, and then with steadily increasing loads until it failed. Various data were collected between and during fatigue loading sessions. The data were measured over multiple frequency ranges using a variety of acquisition equipment, including off-the-shelf systems and specially designed hardware developed by the authors. Modal response, diffuse wave-field transfer functions, and ultrasonic guided wave methods were applied to assess the condition of the wind turbine blade. The piezoelectric sensors themselves were also monitored using a sensor diagnostics procedure. This paper summarizes experimental procedures and results, focusing particularly on fatigue crack detection, and concludes with considerations for implementing such damage identification systems, which will be used as a guideline for future SHM system development for operating wind turbine blades.

Outline

- **CX-100 wind turbine blade**
  - Research blade from SNL
  - 9m, Composite structure
- **Fatigue loading**
  - harmonic excitation
  - ~8.5M cycles to failure
- **Instrumentation**
  - Sensor Arrays
  - Hardware
- **Experimental Data**
  - Diffuse wave-field measurements
  - Ultrasonic Guided waves
- **Experimental Results**
  - Fatigue crack detection performance
  - Sensor diagnostics.
- **SHM system Deployment**

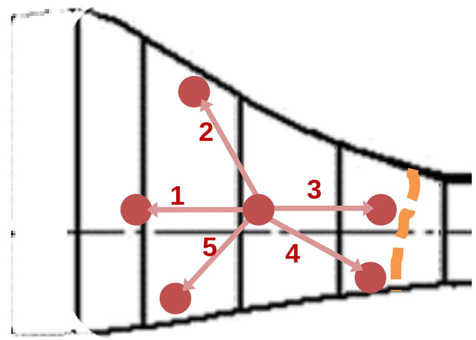

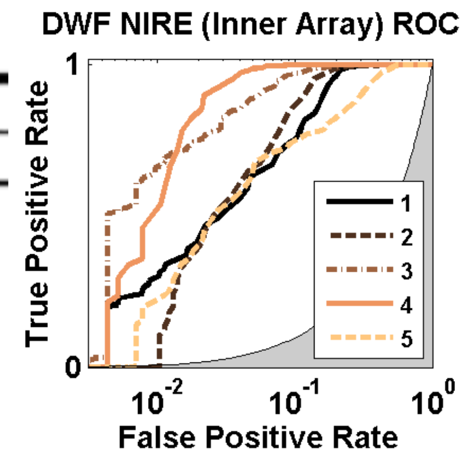

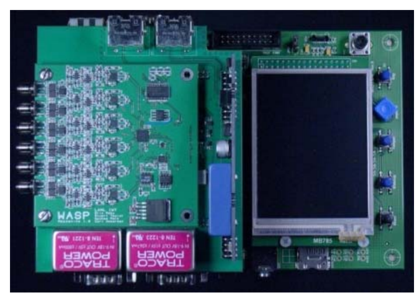

The CX-100 Wind Turbine Blade

- Designed at SNL
- 9-meters long
- Balsa wood frame
- Fiberglass Body
- Carbon Fiber Spar Cap
- Thick root section

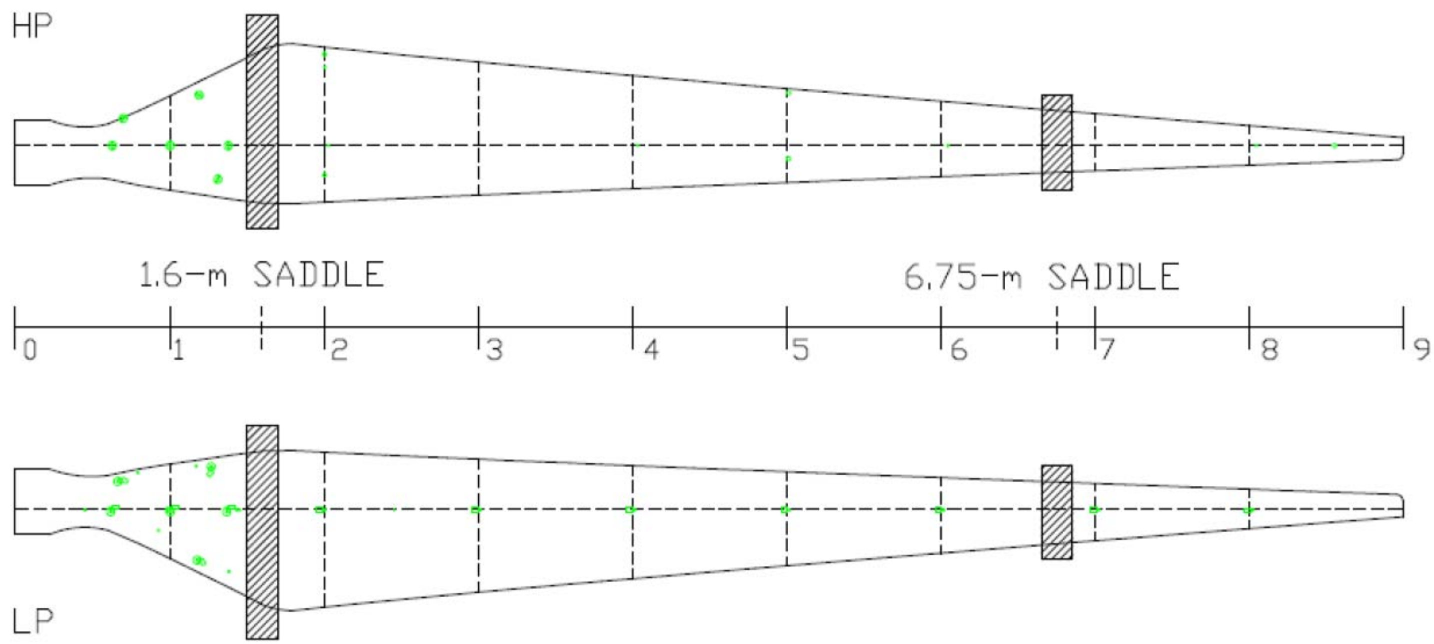

Fatigue Test Operation

- **Fatigue test conducted at NREL's National Wind Technology Center.**
- **Excitation using Universal Resonant EXcitation (UREX).**
- **Moment Distribution Saddles at 1.6m and 6.75m**
- **Excitation at first natural frequency (1.8 Hz)**
- **Multiple Sensing and Diagnostic Systems Deployed**

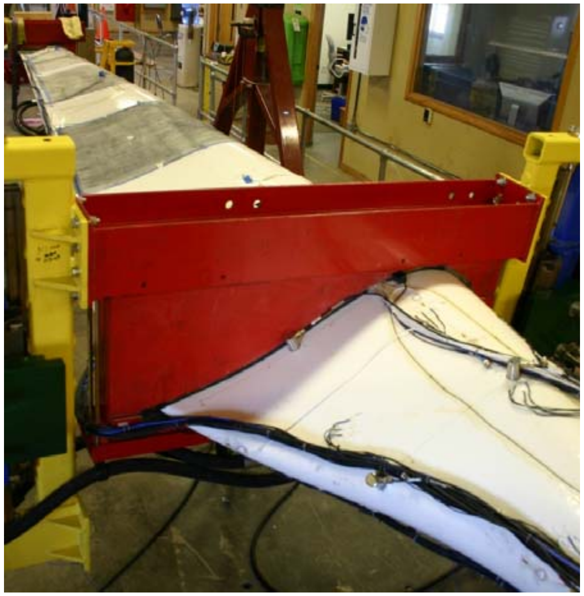

Passive/Diagnostic Sensing Systems

National Instruments - cRIO

- **Passive sensing at 1.6kHz**
  - Accelerometers
  - Piezoelectrics
  - Internal microphone
- **Commercial DAQ for embedded applications**

Sensor Diagnostics (HP4291A)

- **Impedance measurement sweeps from DC to 30kHz**
- **Imaginary part of Admittance can indicate sensor bond condition**
- **Measurements taken approximately once/week**

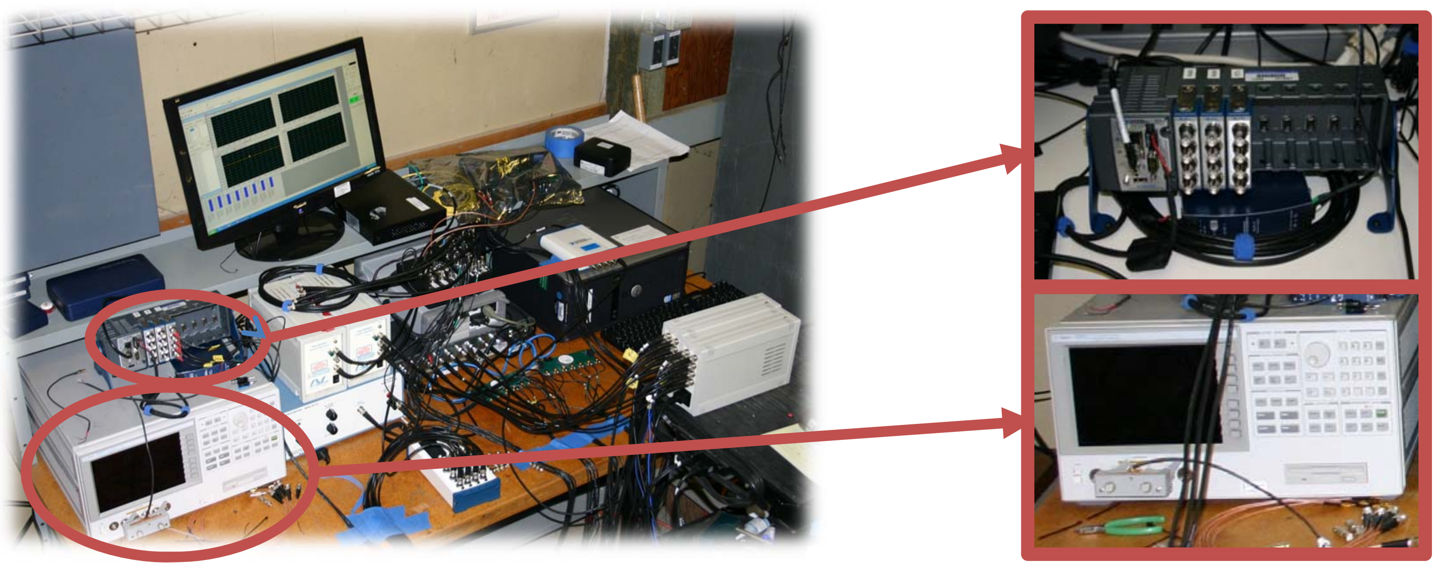

Active Sensing Systems

Ultrasonic Guided Waves

- **Metis IntelliConnector**
  - 10 MHz sampling rage
  - Excited from 50-250 kHz at 25 kHz intervals
  - One sensor array on each blade surface; 0.5-m transmission distances.

Diffuse Wave Fields

- **$\text{LASER}_{\text{USB}}$ by LDS Dactron**
  - White noise excitation from 100 Hz to 40 kHz
  - Two sensor arrays low pressure surface
    - 0.35-m and 1-m transmission distances, respectively
- **Wireless Active Sensing Platform (WASP)**
  - Active/Passive sensing with 100 kHz bandwidth
  - Multiple sensing modes
    - Active, Passive, Impedance
  - Autonomous or web-driven data acquisition
  - Onboard processing power
  - Externally amplified excitation

Sensor Arrays – Low Pressure Surface

- **Active arrays on Low-Pressure Surface**
  - WASP-1
  - Metis-1
  - LASER (Inner, Outer)
- **The inner array observes a 0.75 m diameter region centered 1m from the root**
- **The outer array observes a 2m diameter region 1.5m from the blade root**

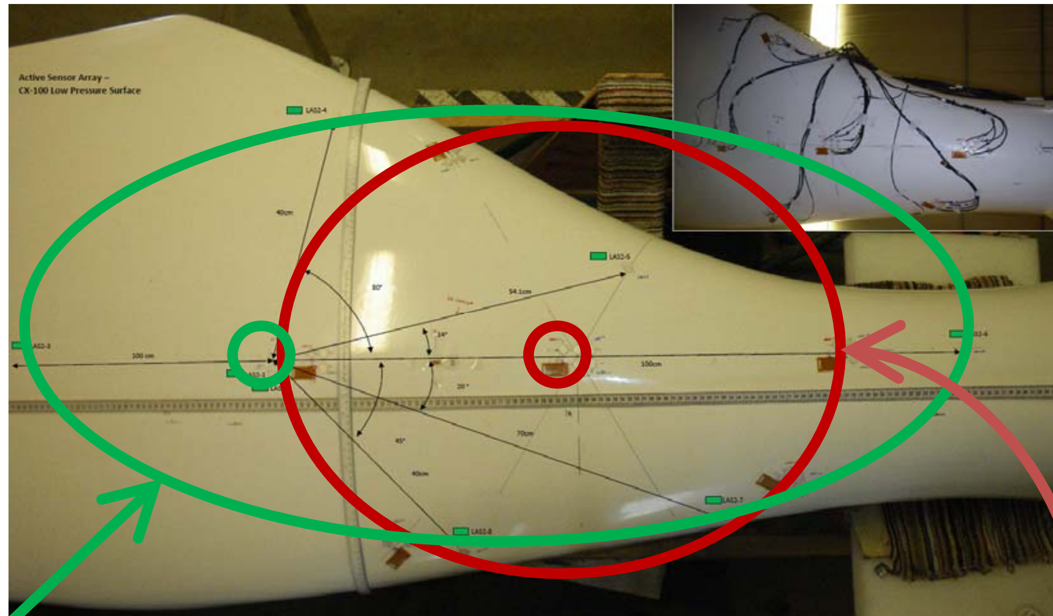

Low pressure surface transitional root area

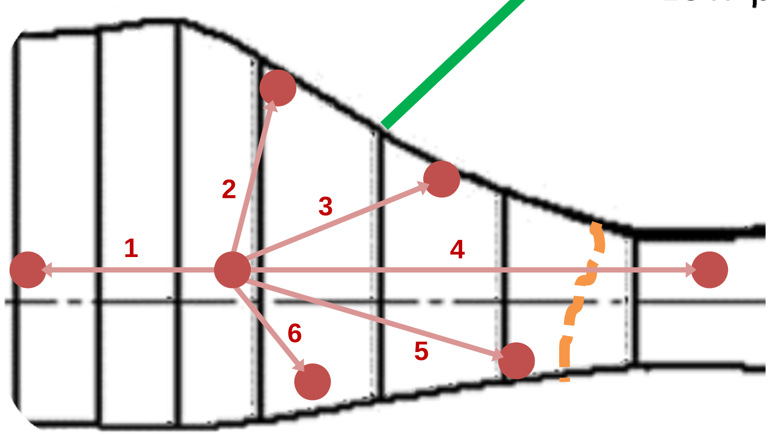

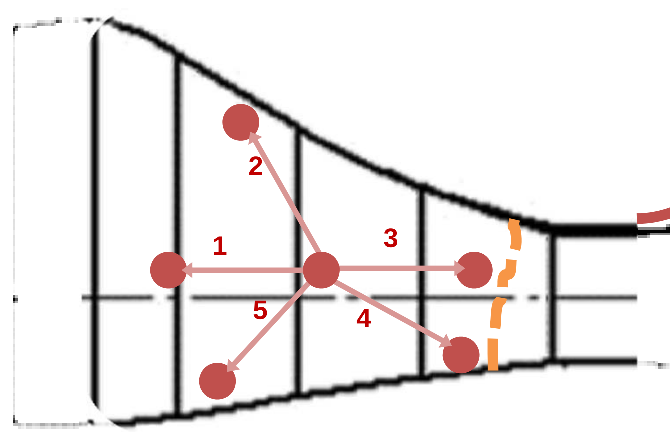

Test Statistics: Guided Waves

- **Match all test waveforms with a baseline waveform minimizing norm of their difference.**
- **Compute each residual as the difference between a waveform and its baseline.**
- **Compute Test Statistics**
  - **Normalized Residual Energy (NRE)**
  - **Correlation Coefficient Complement (CCC)**

$$NRE = \frac{\sum \mathbf{v}_i^{\,2}}{\sum \mathbf{w}_j^{\,2}}$$

$$CCC = 1 - \sum \frac{\left(\tilde{y}_i - \mu_{y_i}\right)\left(\tilde{y}_j - \mu_{y_j}\right)}{\sigma_{y_i}\sigma_{y_j}}$$

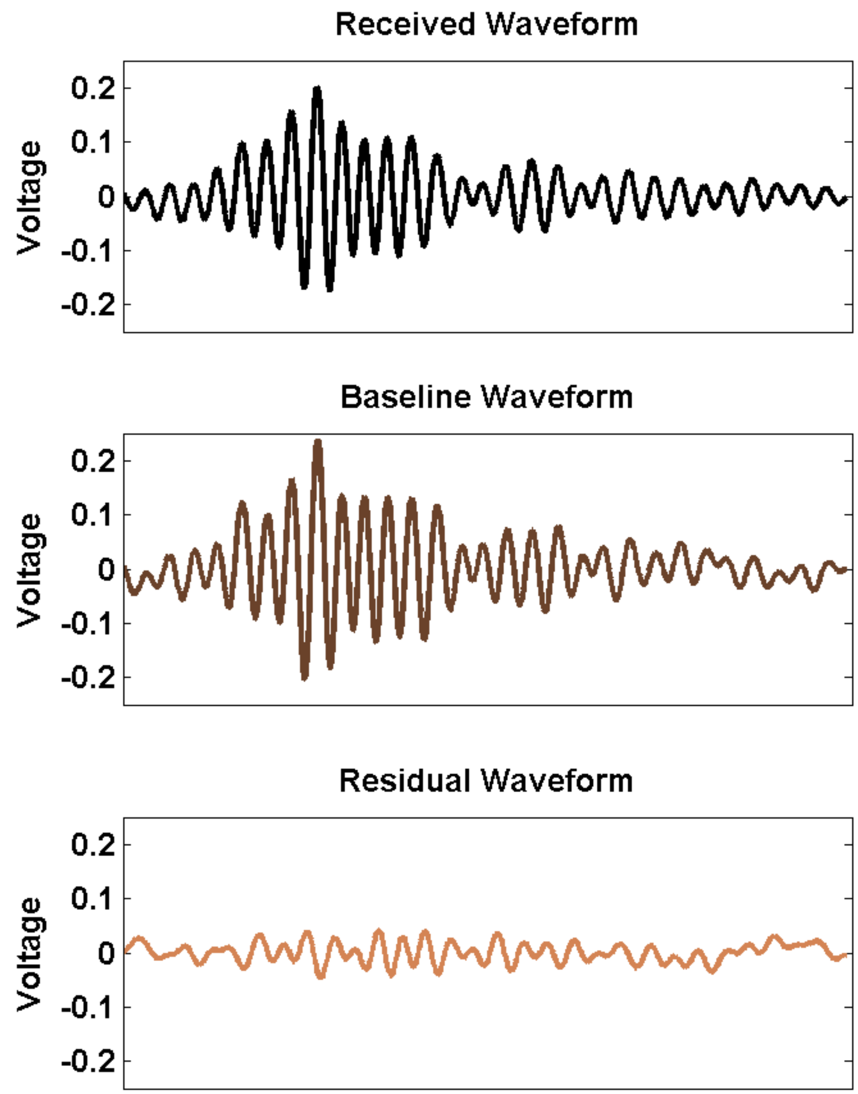

Test Statistics: Diffuse Waves

- **Measurements are colored noise; baseline subtraction produces more colored noise.**
- **Estimate Impulse Response Function (IRF) as iFFT of FRF**
- **Use IRF as test waveforms and compute impulse residual**
- **Compute Test Statistics**
  - **Normalized Impulse Residual Energy (NIRE)**
  - **Impulse Correlation Coefficient Complement (ICCC)**

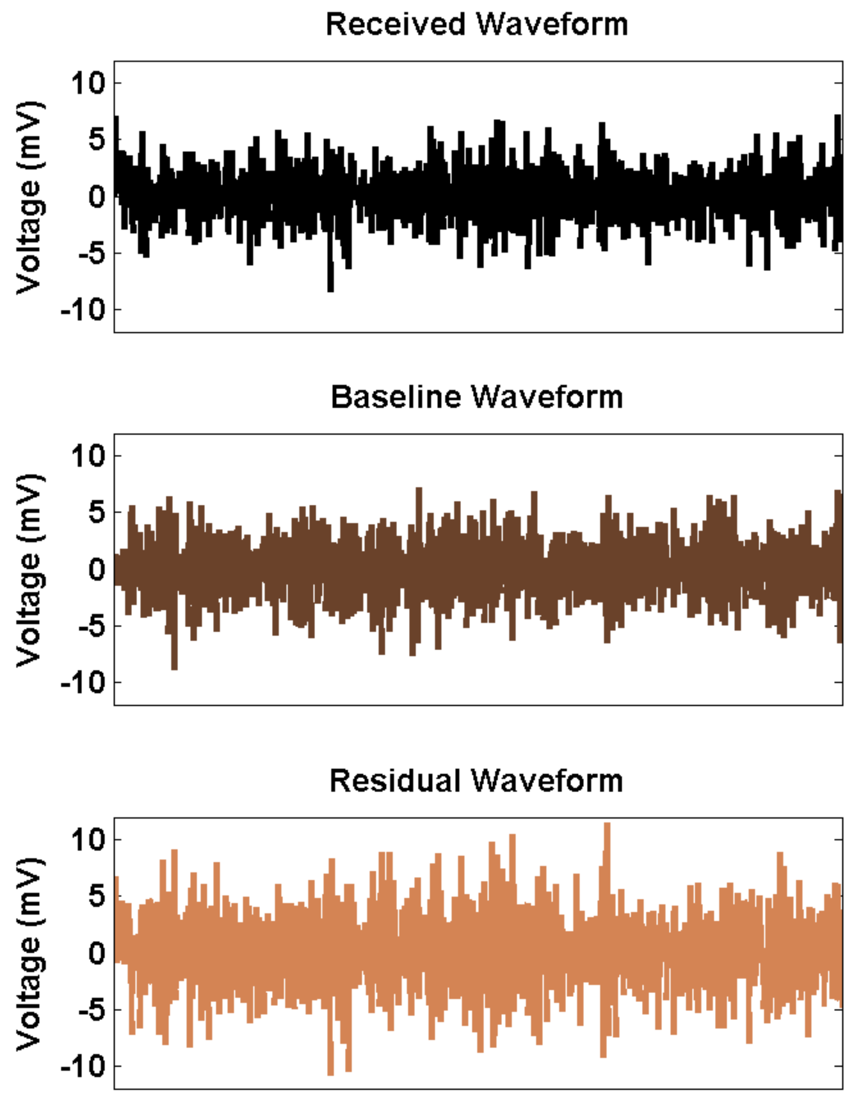

$$NIRE = \frac{\sum \boldsymbol{\upsilon}_i^{\,2}}{\sum \boldsymbol{\omega}_j^{\,2}}$$

$$ICCC = 1 - \sum \frac{\left(\psi_i - \mu_{\psi_i}\right)\left(\psi_j - \mu_{\psi_j}\right)}{\sigma_{\psi_i}\sigma_{\psi_j}}$$

Test Statistics: Diffuse Waves

- **Measurements are colored noise; baseline subtraction produces more colored noise.**
- **Estimate Impulse Response Function (IRF) as iFFT of FRF**
- **Use IRF as test waveforms and compute impulse residual**
- **Compute Test Statistics**
  - **Normalized Impulse Residual Energy (NIRE)**
  - **Impulse Correlation Coefficient Complement (ICCC)**

$$NIRE = \frac{\sum \boldsymbol{\upsilon}_i^{\,2}}{\sum \boldsymbol{\omega}_j^{\,2}}$$

$$ICCC = 1 - \sum \frac{\left(\psi_i - \mu_{\psi_i}\right)\left(\psi_j - \mu_{\psi_j}\right)}{\sigma_{\psi_i}\sigma_{\psi_j}}$$

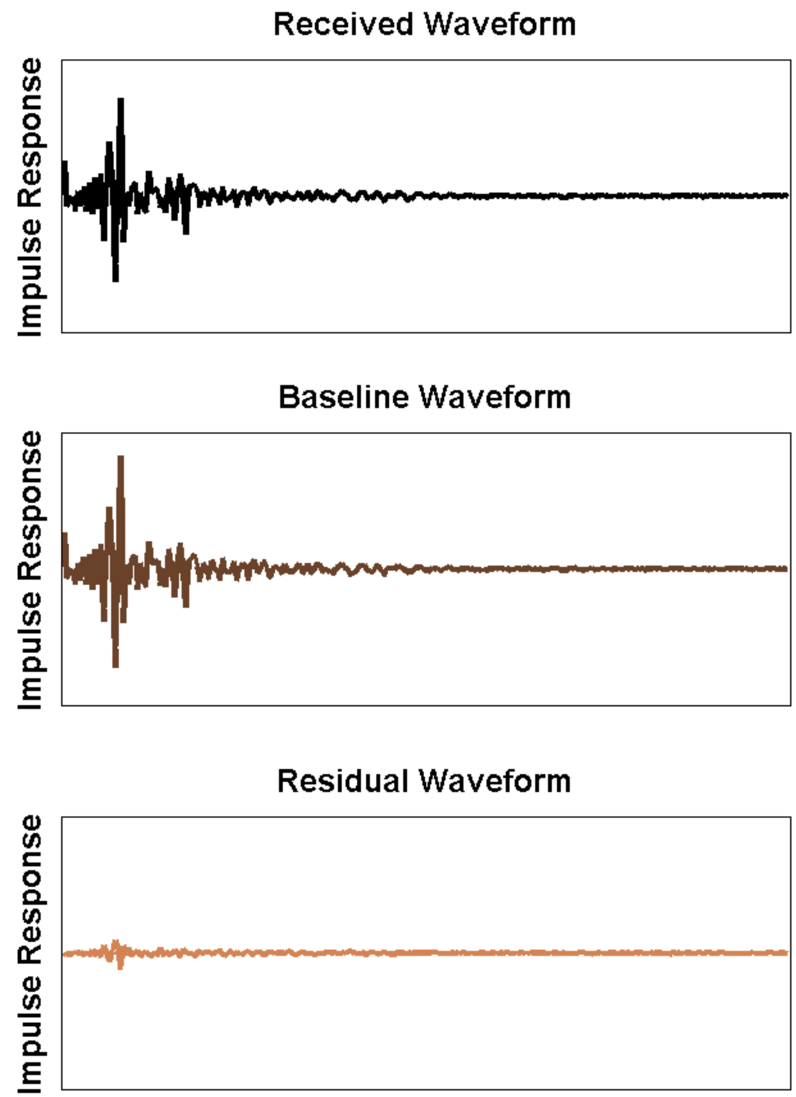

Fatigue Crack Detection Performance

- At 200 kHz, the spar cap may act as a wave guide
- The crack is detectable in either direction (1 or 3)
- Proximity to the crack does not affect the detection performance

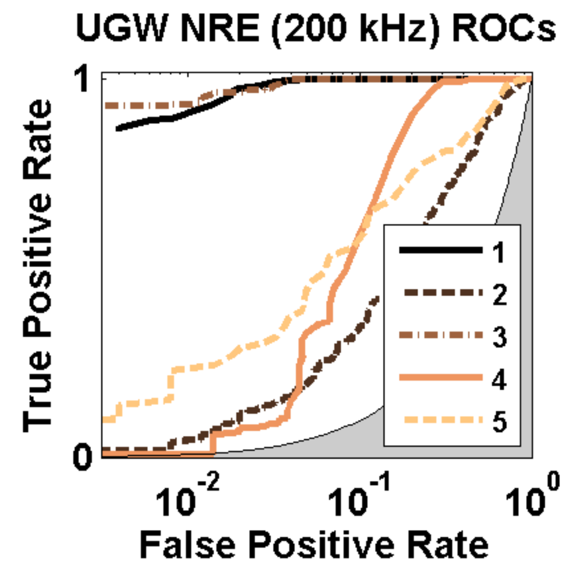

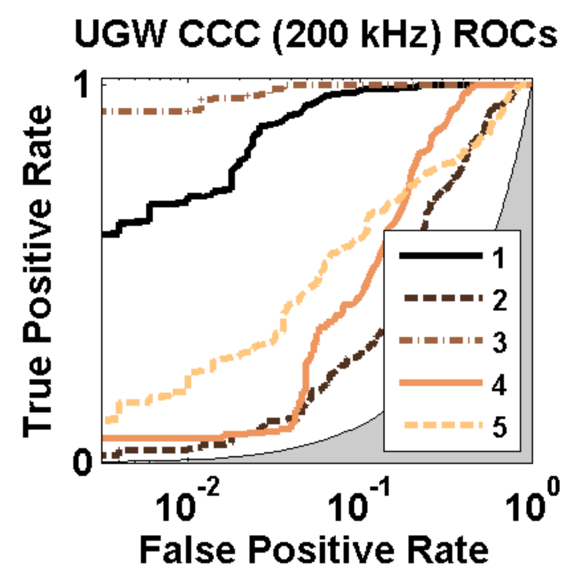

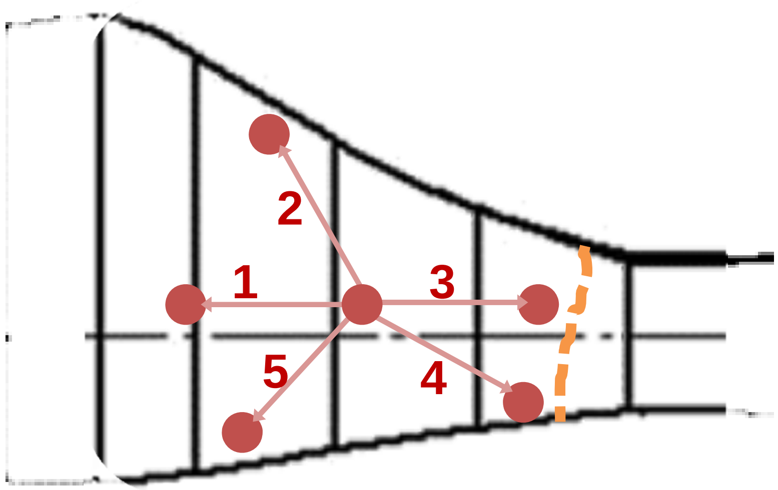

Fatigue Crack Detection Performance

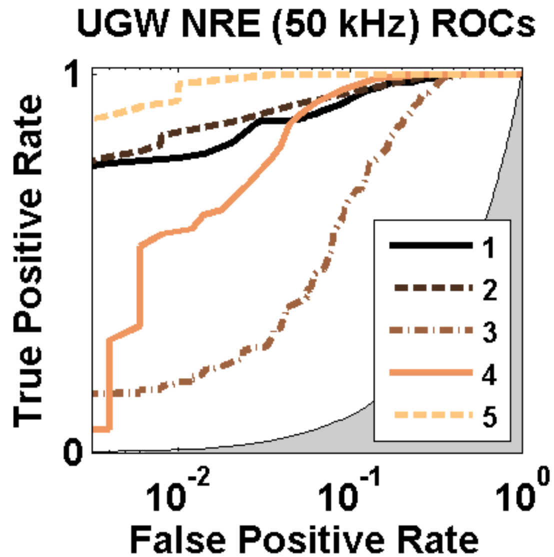

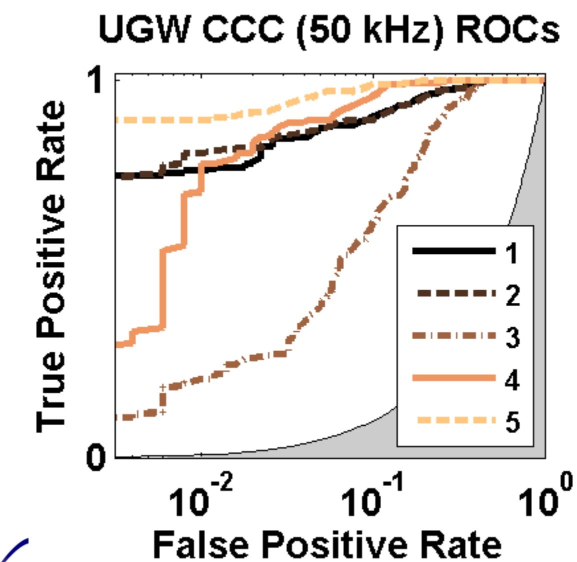

- **At 50 kHz, detection performance with guided waves does not increase with proximity to the crack.**

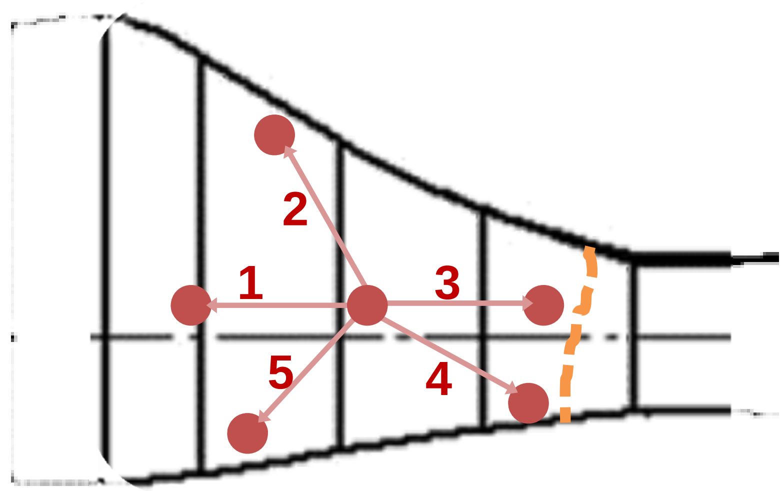

Fatigue Crack Detection Performance

- With the Inner Array, the energy detector has higher sensitivity near the crack.
- The correlation detector has somewhat lower performance.

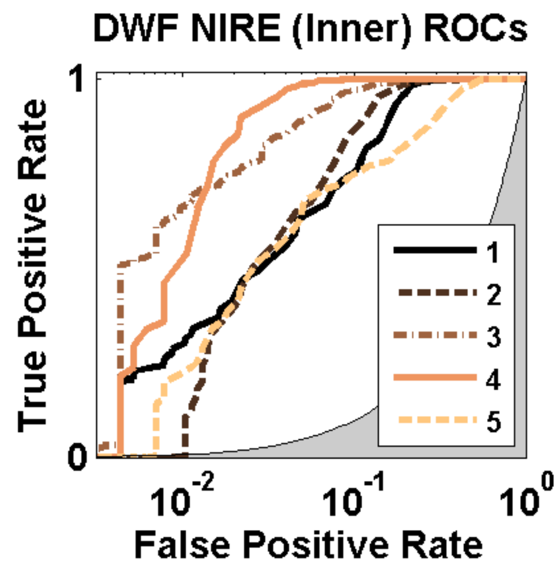

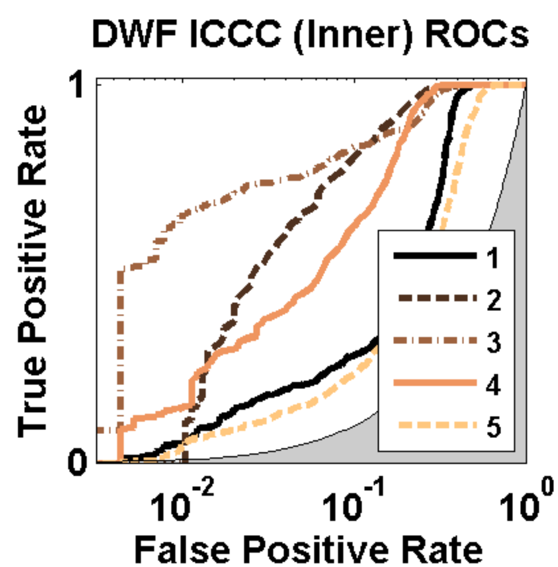

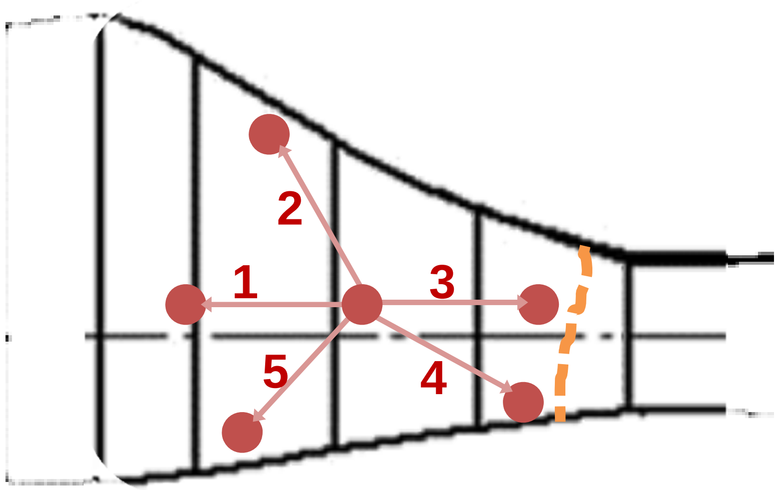

Fatigue Crack Detection Performance

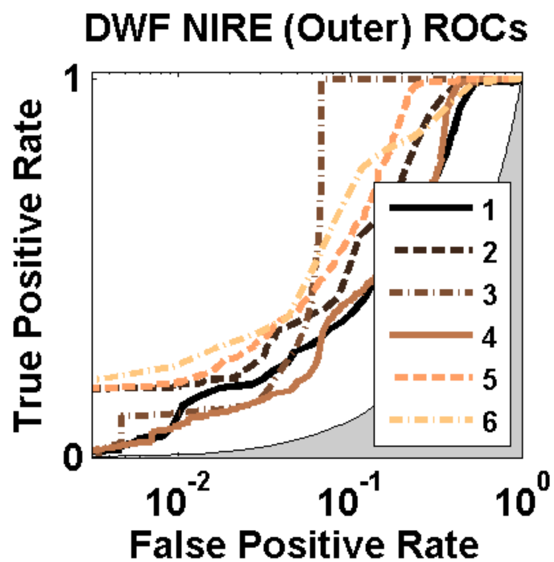

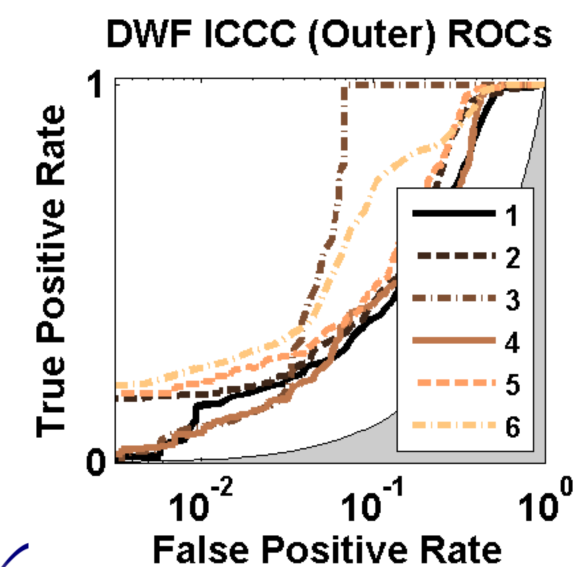

- **The outer array suffers from poor relative performance.**
- **An actuator replacement limits the utility of data after 10/31/11**
  - With the crack forming by 10/20/11, no new baseline for crack detection could be established.

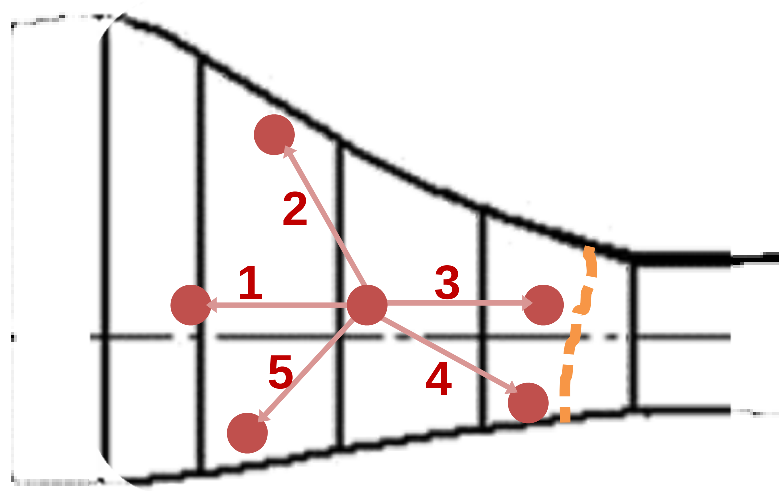

Sensor Diagnostics Overview

- This test utilized circular PZT patches bonded to fiberglass.
- The bonding state of the patches is reflected in their capacitive behavior.
- Changes in that behavior can be inferred from the slope of the imaginary part of the admittance curve.
- An increased slope indicates a more free-free condition.
- A decreased slope indicates a reduction in capacitance, usually a result of breakage.

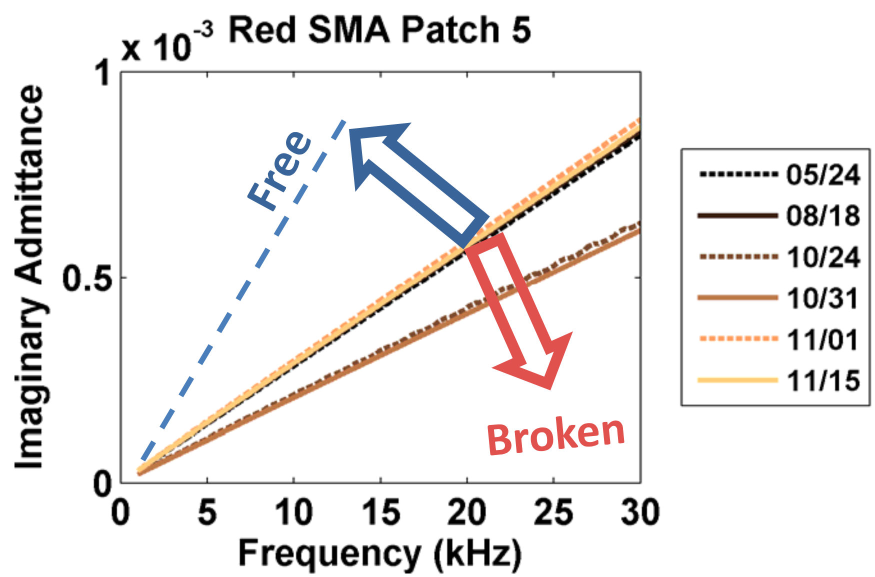

$$Y(\omega) = \frac{I}{V} = i\omega a\left(\bar{\varepsilon}_{33}{}^{T} - \frac{Z_a(\omega)}{Z_s(\omega) + Z_s(\omega)} d_{3x}^{2} \hat{Y}_{xx}{}^{E}\right)$$

Cycle Accumulation and Sensor Failures

- Twelve sensors failed through the course of the test, one of which failed near the test start.
- Many failures were precipitated by the blade's catastrophic failure.
- The majority of failures occurred near the crack (locations LP-3/4).
- Almost all failures, including those at other locations (OL), occurred after the blade had undergone over three times (3x) its rated fatigue life.

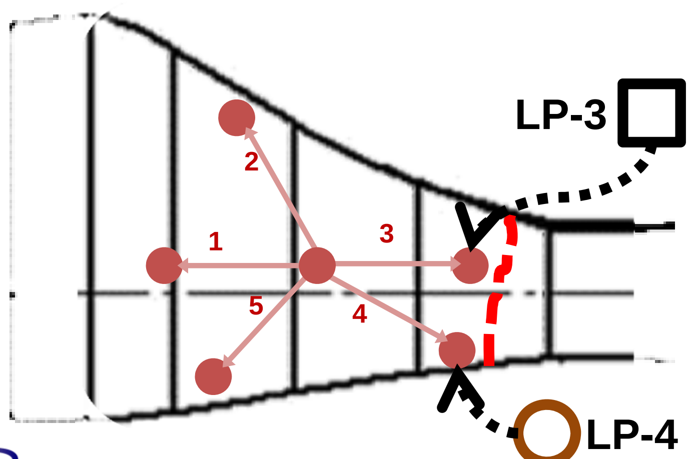

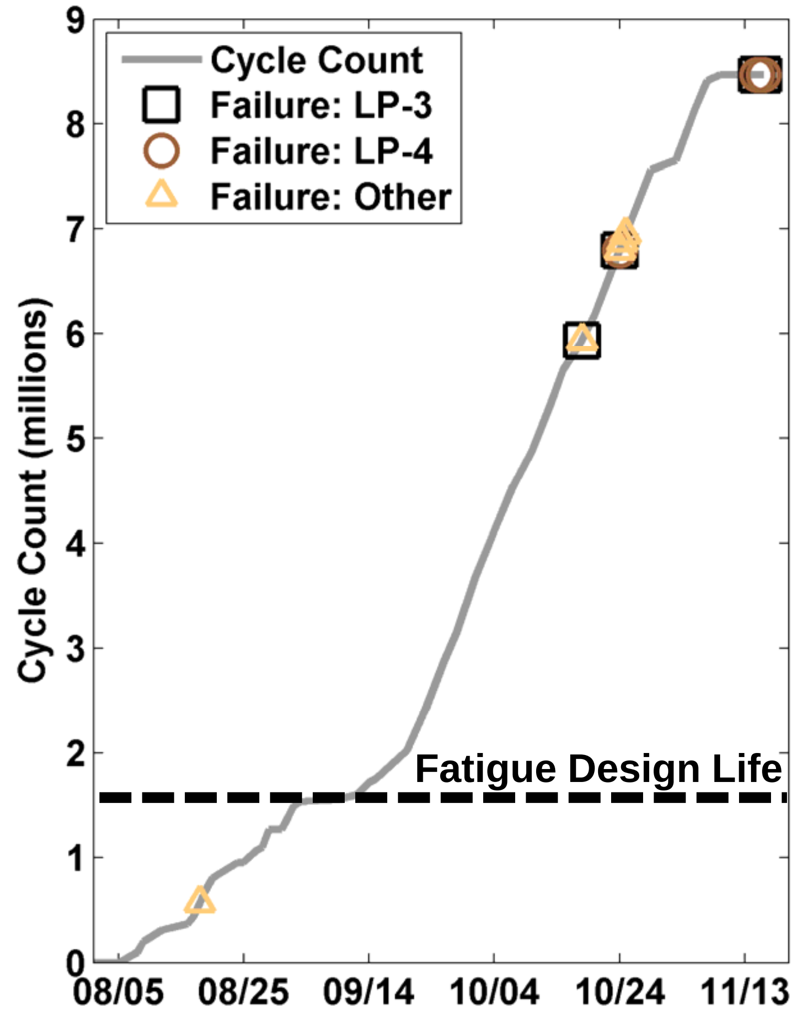

Sensor Diagnostics Overview

NI Active Sensing Array

- **Patch 5 broke early in the test**
  - Some data were collected during fatigue loading
  - First example of breathing crack behavior in this test
  - The patch was not immediately replaced
  - Fully broken behavior was exhibited the next day, following the lower slope
- **Patch 7 remained healthy**
  - This patch sat at 7m, and saw very low strains

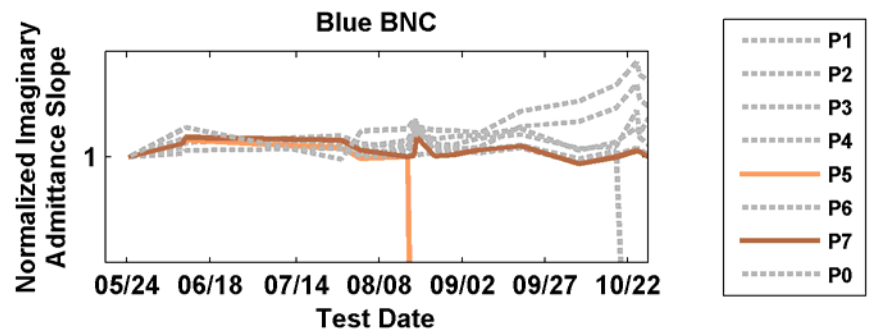

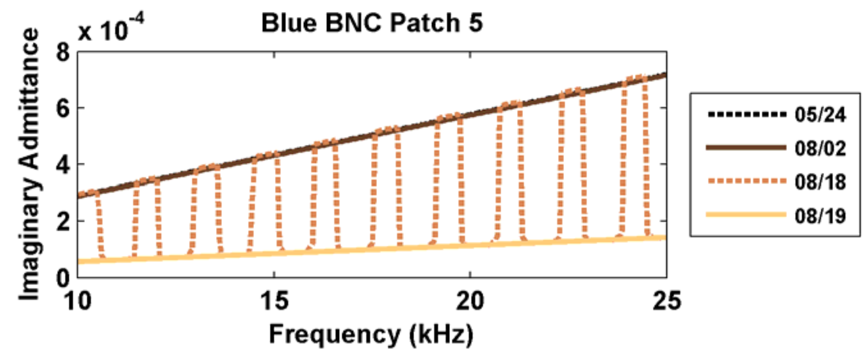

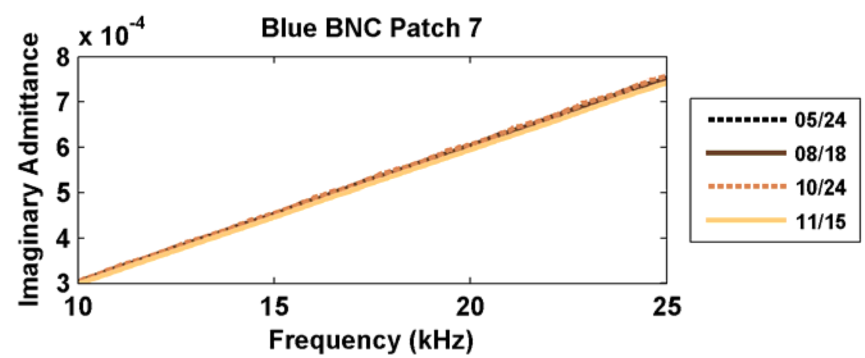

Sensor Diagnostics Overview

WASP LP Array

- **Patch 2 remained healthy.**
  - Some data were collected during fatigue loading
  - Located within 1m of the blade root, this patch saw high fatigue strains.
  - The structural impedance is cyclic for data collected during fatigue loading.
- **Patch 4 sat directly atop the ultimate failure.**
  - As the crack formed, the blade surface softened.
  - This patch was ultimately replaced twice.

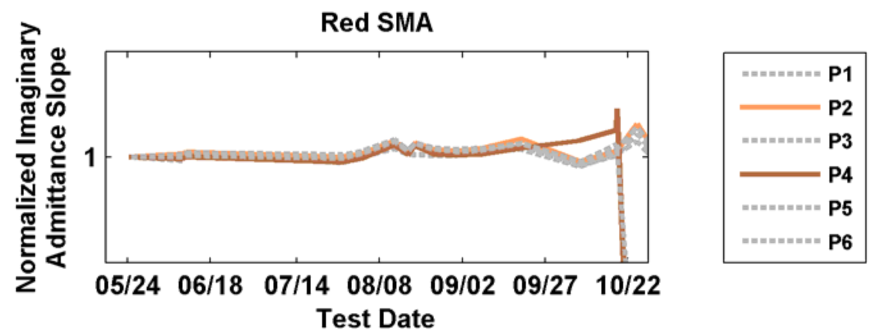

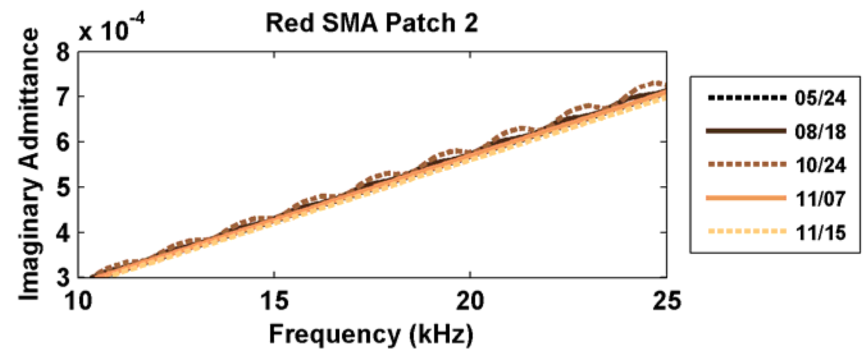

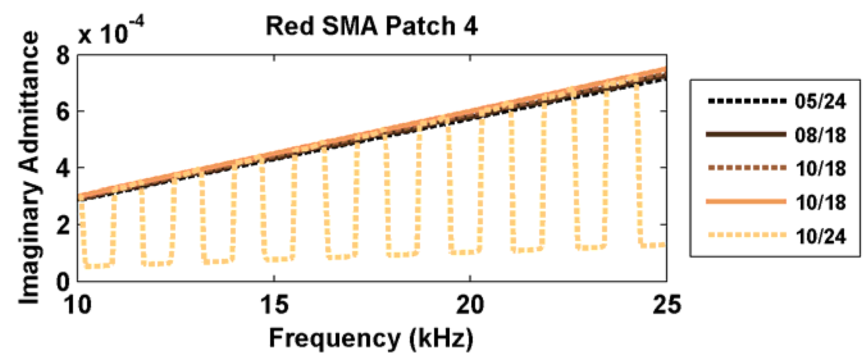

SHM System Deployment

Wireless Active Sensing Platform (WASP)

- Diffuse wave field measurements
- Six (6) software-reconfigureable, simultaneous channels
- Active/Passive sensing with 50 kHz bandwidth
- Autonomous or web-driven data acquisition
- Onboard processing capability
- Currently deployed on a wind turbine in Texas

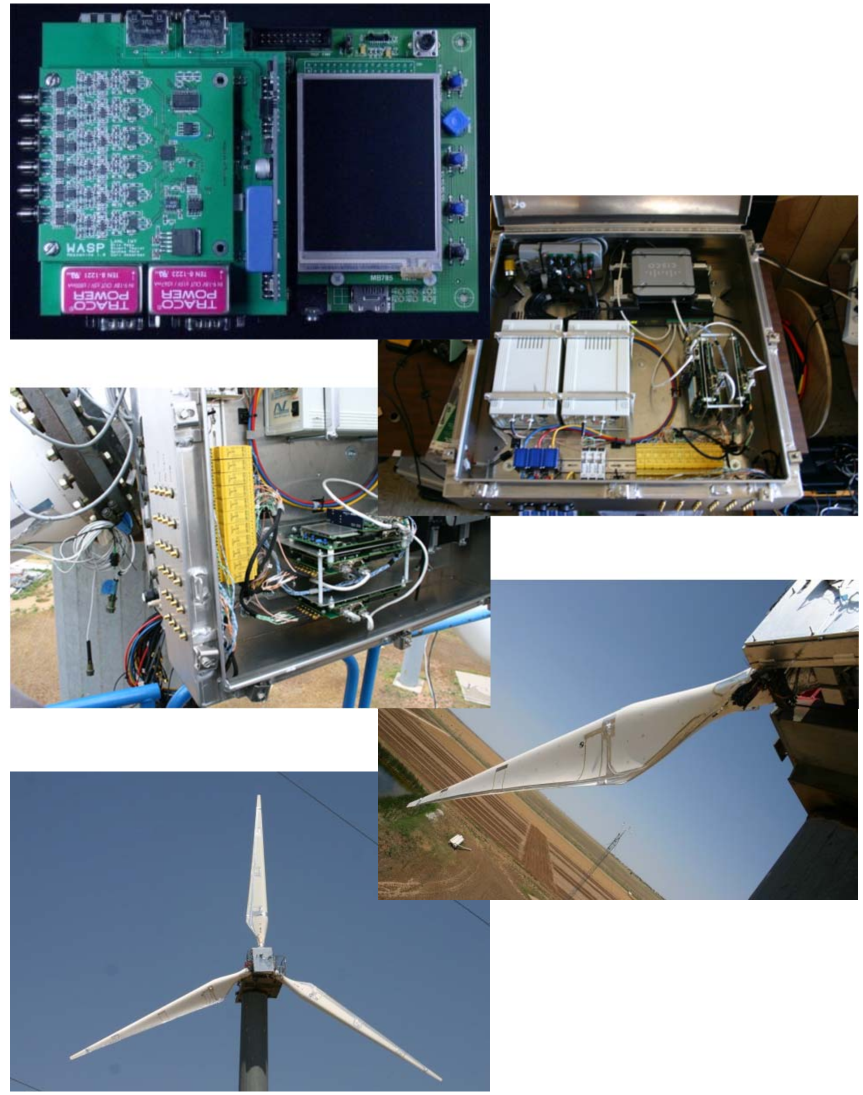

Acknowledgments

- **We would like to thank**
  - Mark Rumsey and Jon White from SNL
  - Scott Hughes and Mike Desmond from NREL
  - Pete Avitabile and Chris Niezrecki from U.Mass, Lowell

for their collaborative support and guidance with this research

- **We gratefully acknowledge the support of the U.S. Department of Energy through the LANL/LDRD Program for this work**
- **This research was also partially supported by the Leading Foreign Research Institute Recruitment Program through the National Research Foundation of Korea funded by the Ministry of Education, Science and Technology (2011-0030065)**